Mechanical Properties of Porous Asphalt Concrete with Rejuvenators

Y. Zhang & M.F.C. van de Ven & A.A.A. Molenaar & M.F. Woldekidan
Road and Railway Engineering, Faculty of Civil Engineering and Geosciences, Delft University of Technology, Delft, the Netherlands

S. Wu
State Key Laboratory of Silicate Materials for Architectures, Wuhan University of Technology, Wuhan, China

ABSTRACT: Preventive maintenance using rejuvenators to extend the service life of porous asphalt pavements has been investigated recently in the Netherlands. Three rejuvenators (one bituminous binder and two emulsions) were applied in two test sections on motorways. In this paper the mechanical properties of porous asphalt concrete with rejuvenators are investigated using a three-point bending test combined with finite element (FE) modeling. Nano Computed Tomography (CT) is used to scan the internal microstructure of porous asphalt cores to research the distribution of the rejuvenators. The bending stiffness is determined by using a surface-up (rejuvenated area is located at the top of the beam) and a surface-down (rejuvenated area is at the bottom of the beam) mode to investigate the increased flexibility of porous asphalt concrete with rejuvenators. Two dimensional FE models of a single-layer porous asphalt (SLPA) beam and a two-layer porous asphalt (TLPA) beam are used to analyze the experimental data. The results of the investigation indicate that rejuvenators not only soften the aged mortar but also supply extra bonding within the porous asphalt concrete. The bending stiffness of the porous asphalt beam increased when rejuvenators were applied.

KEY WORDS: Porous asphalt, rejuvenator, bending stiffness, Nano CT scan, FE modeling.

1 INTRODUCTION

Porous asphalt concrete is extensively used as a surface layer on motorways in the Netherlands. Due to raveling (loss of aggregates from the pavement surface), the service life of porous asphalt pavement is limited when compared to the life of dense asphalt wearing courses (Van der Zwan et al. 1990, Swart, 1997). Preventive maintenance through addition of rejuvenators is being considered as a cost-effective and environmentally sustainable strategy designed to extend the life of existing pavements.

A literature review showed that researches of rejuvenators focus on two main directions: the preservation technology of the asphalt pavements and the rehabilitation technology in recycling of asphalt pavements. The Texas Department of Transport (TDT) reported a study showing that the rejuvenators penetrated the top 3/8 inch of the surface and increased the flexibility of the mixture. The TDT recommended the application of rejuvenators on asphalt concrete surface layers with a void content greater than 7 to 8 percent. It was shown that the rejuvenators can reduce the stiffness of the mixture (Estakhri, et al. 1991). Benefits of rejuvenators were also reported by Boyer R.E.. He showed that rejuvenators did increase the penetration and decrease the viscosity of asphalt binder in the top portion of the pavement. In

that way, the pavement's life cycle was extended. The rejuvenator increased also the durability of asphalt binder in the top of the pavement by improving the balance of chemical fractions of asphalt binder (Boyer, 2000). Chiu C.T. reported that three rejuvenators applied on a parking lot pavement appeared to penetrate into the pavement to a depth of no more than 2 cm. All rejuvenators showed a considerable softening effect on the old asphalt binders in the top 1 cm of the treated pavement (Chiu, et al. 2006). However, the research results mentioned above are based on the studies of rejuvenators on dense asphalt pavements. Researches of the effect of rejuvenators on porous asphalt pavements are still rare. Expected benefits of rejuvenator to prolong the life of porous asphalt pavements have not been substantiated with quantitative studies. It is likely that fog seals (rejuvenators) prolong the life of porous asphalt pavements, at least marginally, by adding a small amount of un-aged bitumen to the surface of the mix (Rogge, 2002, Cooley et al. 2009). Research also showed one of the disadvantages of rejuvenator on porous asphalt being a temporary loss of friction on pavement and a reduced air voids content; this lower voids content reduced the permeability and functionality of the porous asphalt wearing course (Qureshi, et al. 2011).

Given the limited amount of research done in this area, the Dutch Ministry of Transport has launched a project to research a maintenance method using rejuvenators to extend the service life of porous asphalt. The project was entitled as "Lifetime Extension Maintenance of Porous Asphalt (LVO-ZOAB in Dutch). Field trials were made in which different types of rejuvenators were sprayed on test sections. Cores were taken from the porous asphalt concrete wearing course and were used for experimental research at Delft University of Technology.

2 EXPERIMENTAL PROGRAMME

2.1 Materials

Two test sections on two Dutch motorways (A50 and A73) with heavy traffic were maintained with rejuvenators in 2010. They were both 5 years in service and still in good condition when the rejuvenators were applied. The wearing course of the A50 motorway (located from 190.7 km to 192.7 km) is a Dutch single-layer porous asphalt (PA) 0/16. The bituminous binder used for the construction in this section was a Pen 70/100 bitumen at an amount of 5.5% by weight on 100% aggregates. The wearing course of the A73 motorway (between 100.1 km to 101.5 km) is a Dutch two-layer porous asphalt consisting of a 25 mm top layer of PA 4/8 and a 45 mm bottom layer of PA 11/16. The bituminous binder in the top layer of this section was a SBS modified bitumen.

Three rejuvenation products were supplied by three contractors available for the LVO project. Rejuvenator A is a bitumen emulsion, which was sprayed on the pavement at ambient temperature. Rejuvenator B is a bituminous polymer modified binder, which was sprayed on the pavement at a temperature of 180 ^{o}C. Rejuvenator C, sprayed at a temperature of 70 ^{o}C, is also bitumen emulsion. Small crushed sand or glass particles were sprayed on the pavement after the application of rejuvenators in order to increase the skid resistance. Porous asphalt cores with a diameter of 150 mm were drilled from the test sections on the pavement for the laboratory tests. Specimens from the reference wearing course (without treatment of rejuvenator) were also taken for comparison.

2.2 Test method

A three point bending test was performed for measuring the stiffness of porous asphalt beams. The Single-Layer Porous Asphalt (SLPA) beams and Two-Layer Porous Asphalt (TLPA) beams were sawn from the center of the porous asphalt cores from motorways A50 and A73.

Figure 1 shows a sketch of the beam and the small core from a large core. Dimensions of the SLPA beams are 150 mm in length, 50 mm in width and 40 mm in height. For the TLPA beams, only the height is changed to 25 mm. The beams were subjected to the haversine force using frequency sweeps between 0.1 and 4 Hz at a temperature of 5 ^{o}C. Applied loads for SLPA beams and TLPA beams are 100 N and 60 N, respectively.

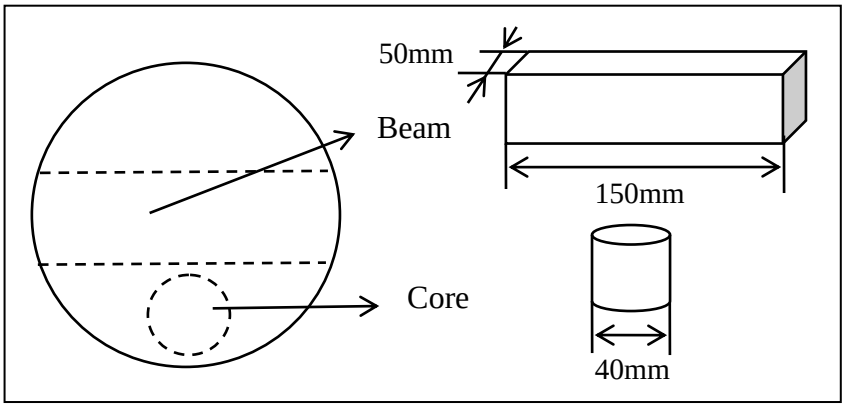

Figure 1: The sketch of the beam and the small core from a large core

For the bending test, the results of the bending stiffness E are corrected using a shift factor κ as shown in Equation (1). It is necessary as the deflection due to shear can't be neglected compared to the deflection due to bending moment *I*. Generally, it is recommended that the effective length *L* should not be less than six times whatever the highest value is for the width or the height (EN 12697-26: Stiffness).Therefore, two shift factors obtained from the SLPA beam model and TLPA beam model (Section 3.1) are used to calculate the bending stiffness.

$$E = k \cdot \frac{PL^3}{48 \cdot \delta_{max} I} \tag{1}$$

As shown in Figure 2, two test modes are implemented in the bending test. Due to the penetration depth of rejuvenators, the upper part of the beam (in the as-built orientation) is the rejuvenated area (Section 4.1). In the surface-up mode, the rejuvenated area is located at the top of beams. In the surface-down mode, the rejuvenated area is located at the bottom.

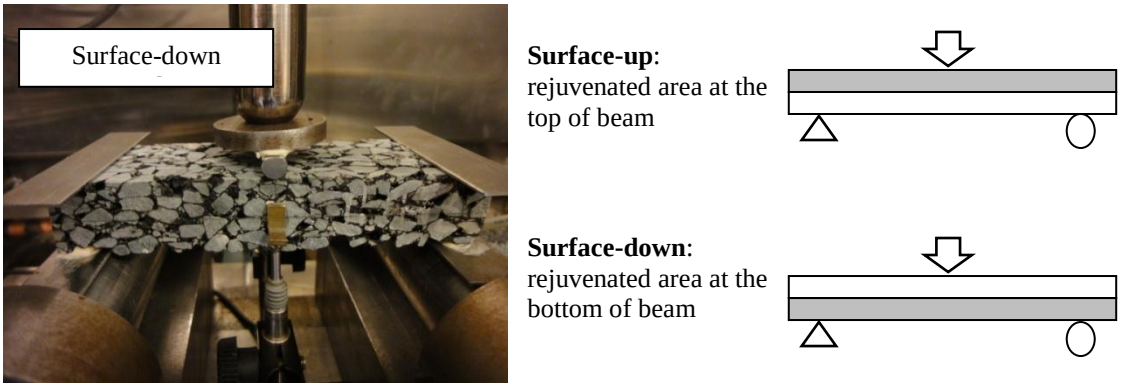

Figure 2: A test picture of the three-point bending and schematic diagram of two test modes

Nano Computed Tomography (CT) scanning was performed on small porous asphalt cores using a Phoenix Nanotom Scanner to detect the internal microstructure. The Nano CT system

consists of a high power nanofocus X-ray source, a precision object manipulator, a high resolution CCD detector and a computer for control and reconstruction. The source is an open X-ray tube with detail detectability of 0.2-0.3 microns. The object manipulator is composed of three linear motion stages for magnification adjustment (X), alignment (Y), positioning (Z) and rotating motion stage (θ) for sample rotation. Digital geometry processing is used to generate a three-dimensional image of the inside of an object from a large series of two-dimensional X-ray images taken around a single axis of rotation.

Small porous asphalt cores with a diameter of 40 mm and a height of 25 mm were drilled from the same cores from which the beams were taken (as shown in Figure 1). The test procedure and sample preparation method that were used in the Nano CT scanning have been described in detail previously (Verwaal, 2011). The scanning was progressed with a slice distance of 0.04 mm and a resolution (voxel size) of 0.04 mm.

3 MODEL CHARACTERISTICS

3.1 Model restraints

From the computed tomography scanning images of the porous asphalt cores, three main material components can be discriminated being the aggregate particles, the mortar and the air voids. Finite element meshes, for analyses of the beams by means of ABAQUS, of a SLPA beam and a TLPA beam in ABAQUS were created from the X-ray images. Figure 3 shows a mesh of the TLPA beam model in the three-point bending test.

In this two dimensional beam model, a thin steel plate was placed at the end of the beam bottom for the support. For the bending test, steel plates were glued in order to get a stabilized and hard contact at the support. Two contact interactions properties between steel plates and the supports in the model were defined for smoothly bending of beam. At left side, the tangential behavior of the nodes is rough (only rotation allowed). At right side, the tangential behavior is frictionless, which means the nodes of steel plate can slide on the surface of the right support (As shown in the enlarged images in Figure 3).The boundary conditions of this model were defined in the nodes located at the bottom of the two supports, where displacements in the horizontal and vertical direction were restrained. No displacements perpendicular to the plane of the model were allowed.

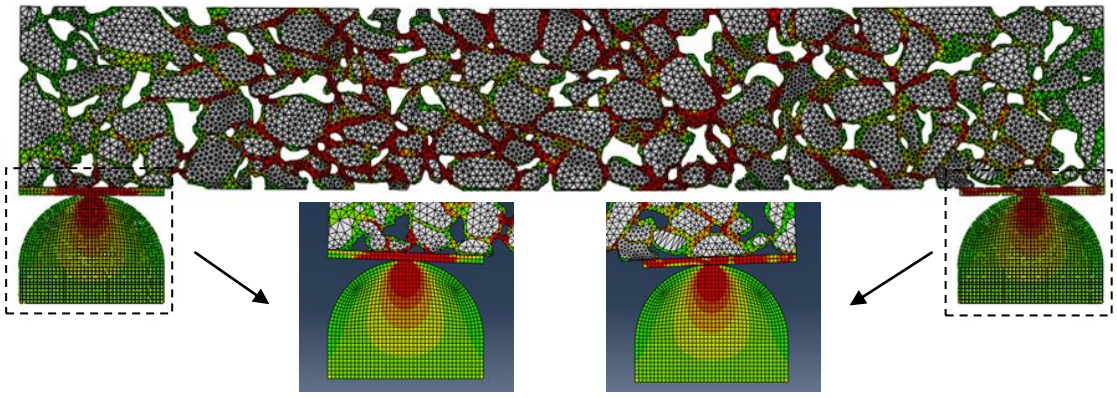

Figure 3: The TLPA beam model in the bending and its interactions at the supports

The first analyses were focused on quantifying the influence caused by the dimensions of beams. In this analysis the beam was modeled as a homogeneous elastic beam and the maximum deflection obtained with ABAQUS was compared with the results of analytical

solution. Equation 1 was used for the analytical solution. Using the regression function, shift factors for SLPA beam model and TLPA beam model were determined. As shown in Figure 4, the shift factor of SLPA beam mode is higher than TLPA beam model. It's logic that deflection caused by shear stress is less in beam model with a higher length/height's ratio.

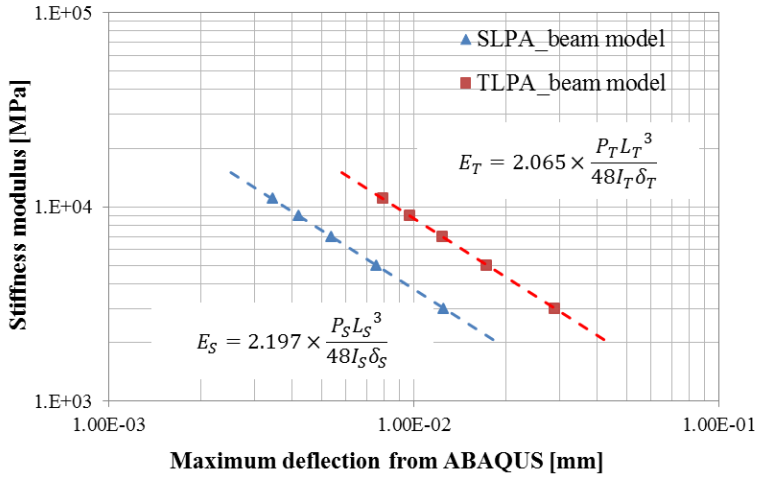

Figure 4: Stiffness modulus vs. the deflection with shift factors

3.2 Material behavior

In both the SLPA beam model and TLPA beam model, the aggregates were modeled as linear elastic with a modulus of 30 GPa and a Poisson's ratio of 0.20. The steel plates of the supports were modeled as linear elastic with a modulus of 200 GPa and a Poisson's ratio of 0.27. The mortar was modeled by a modified Huet-Sayegh (MHS) model implemented in ABAQUS.

In the MHS model a linear dashpot is placed in series with the original HS model. This improves the low frequency region fit of the model to master curve data (Woldekidan et al, 2012). The mathematical expression of the MSH model in frequency domain is given by Equation (2).

$$J^*(\omega)_{MHS} = \frac{G'}{|G^*(\omega)|^2} - i\left[\frac{G''}{|G^*(\omega)|^2} + \frac{1}{\eta_3 \omega}\right] \quad (2)$$

In Equation (2), $J^*(\omega)_{MHS}$ denotes the creep compliance of the MHS model, G', G'' and $|G^*(\omega)|$ denote the expression for the storage modulus, loss modulus and magnitude of the complex shear modulus for the original HS model (Pronk, 2005). The parameter η_3 is the linear dashpot parameter. The MHS model parameters for the SBS modified mortar at a temperature of 5 ^oC were determined and reported by Woldekidan. The parameters from master curve of this mortar are listed in Table 1.

Table 1: WLF factors and MHS model parameters for the SBS modified mortar at T_{ref} = 5 ^oC

	WLF factors		MHS model parameters						
SBS modified mortar	C_1	C_2	m_1	m_2	δ_1	τ [s]	G_∞ [MPa]	G_0 [MPa]	η_3 [MPa]
	24.35	129.00	0.21	0.60	4.22	0.1133	2333	0.2	8.36E+5

For the mortar a viscoelastic model based on the Prony series representation is utilized (Woldekidan, 2012). The time domain relation for the mortar's model is given in Equation (3). The parameters G_r, G_i and τ_i denote the rubbery shear modulus, the shear stiffness and the relaxation time respectively. For determination of these parameters regression analysis on the data representing master curve was performed. Table 2 lists the Prony series model parameters for the mortar. These were used as input in ABAQUS.

$$G(t) = G_r + \sum_{i=1}^{n} G_i \cdot e^{-t/\tau_i} \quad (3)$$

Table 2: Prony series model parameters for the SBS modified mortar at T_{ref} = 5 °C (12 terms)

Mortar		Model parameters					
SBS modified mortar	G_0 [MPa]	1796.9					
	τ_i [s]	3.32E-6	2.86E-5	2.47E-4	2.12E-3	1.83E-2	1.58E-1
	α_i [-]	1.60E-1	2.05E-1	1.14E-1	1.58E-1	1.23E-1	1.06E-1
	τ_i [s]	1.36E+0	1.17E+1	1.01E+2	8.68E+2	7.48E+3	6.45E+4
	α_i [-]	7.50E-2	3.84E-2	1.32E-2	3.97E-3	9.80E-4	3.63E-4

The material properties of a soft bituminous binder were used to represent the behavior of the rejuvenator in the beam model. The master curve of this binder was described using parameters of the Christensen Anderson (CA) model (Christensen and Anderson, 1992). Table 3 gives the parameters for the master curve of soft binder.

$$|G^*(\omega)| = G_g \left[1 + \left(\frac{\omega_c}{\omega}\right)^{\frac{\log 2}{R}}\right]^{\frac{-R}{\log 2}} \text{ and } |\delta(\omega)| = 90 \left[1 + \left(\frac{\omega}{\omega_c}\right)^{\frac{\log 2}{R}}\right]^{-1} \quad (4)$$

In Equation (4), $|G^*(\omega)|$ denotes the magnitude of the complex shear modulus. $\delta(\omega)$ denotes the phase angle. G_g is the glassy modulus. ω_c is the location parameter. ω is reduced frequency. R is the rheological index.

Table 3: WLF factors and CA model parameters for the soft binder at T_{ref} = 5 °C

	WLF factors		CA model parameters		
Soft binder	C_1	C_2	R	Gg [Pa]	ω_c[rad/s]
	27.28	160.78	1.719	1.0E+09	0.0259

4 RESULTS AND DISCUSSION

4.1 Volumetric properties of porous asphalt cores

After the reconstruction of the scanning data, two dimensional X-ray images can be created. The two dimensional X-ray images contain information about the position and density of the segmented components within the sample. In the image (a) of Figure 5, three components can be distinguished in the reference porous asphalt core, which are aggregates, mortar and air voids. The voids content over the height of porous asphalt cores can be calculated from the top view images. Results of 10 cores from the reference sections of SLPA show an average

voids content of 11.9% in the top 15 mm. The average voids content of 6 reference cores from TLPA is found to be 17.9% in the top 20 mm. As shown in the image (b), there is no visible difference between this treated core with rejuvenator A and the reference core. But the calculated results show an average voids content of SLPA with rejuvenator A is 10.4% and TLPA with rejuvenator A is 16.0%. This is indicating the presence of rejuvenator A in the porous asphalt cores.

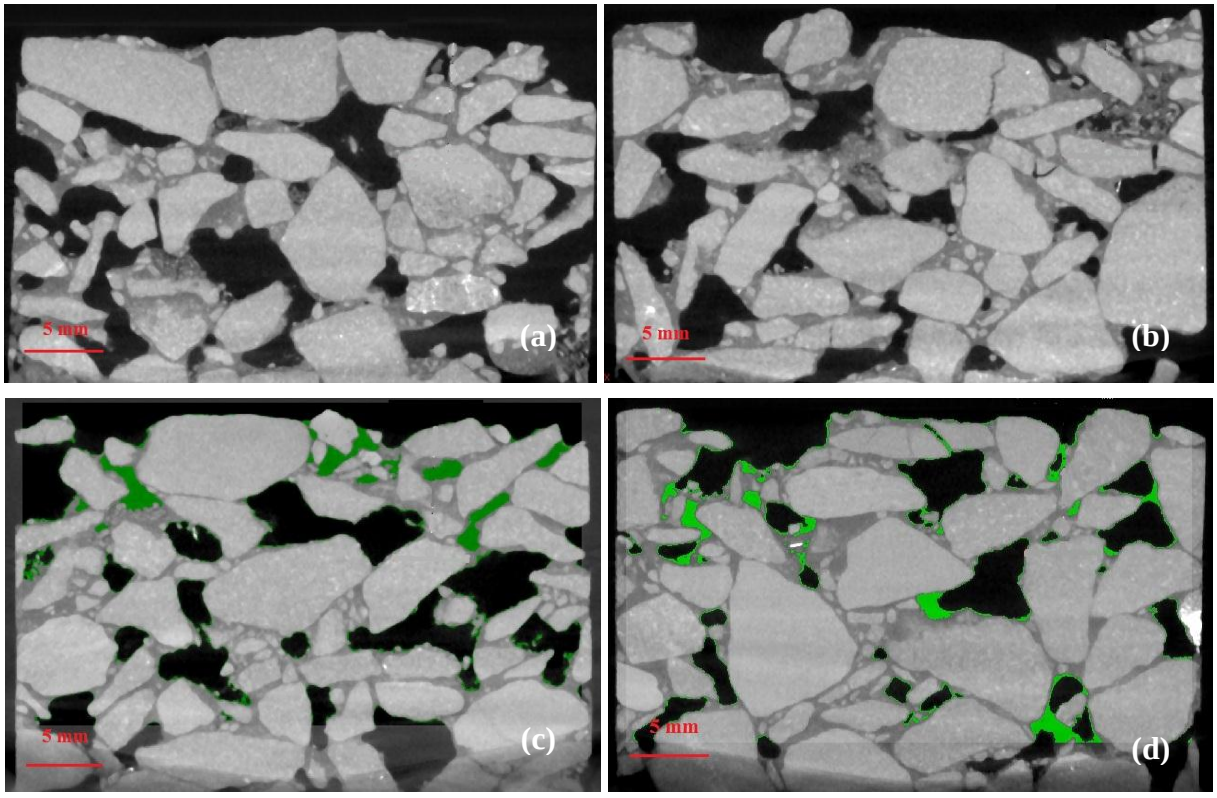

Figure 5: X-ray images (front view) of TLPA in top 25 mm using Nano CT scanning: (a) the reference core; (b) treated with rejuvenator A; (c) treated with rejuvenator B; (d) treated with rejuvenator C

The X-ray images of the cores treated with rejuvenator B and C show different pictures. A fourth component was marked with green color in images 5(c) and 5(d). This component has a lower density than the mortar but a higher density than air voids and is indicating the presence of rejuvenator B and C. The X-ray images show that the distribution of rejuvenator B is mainly in the top 10 mm of porous asphalt cores. However, rejuvenator C did penetrate to a depth of 20 mm in the porous asphalt cores.

4.2 Bending stiffness

The results of the bending stiffness show a wide variation due to the different locations of beams in the pavements. Even beams taken from the left wheel path and the right wheel path in the same location show different results. The average values of bending stiffness in surface-down and surface-up mode of SLPA beams are shown in Figure 6. These results are calculated from 10 reference beams, 6 treated beams with rejuvenator A, 2 treated beams with rejuvenator B and 4 treated beams with rejuvenator C.

It is observed that the bending stiffness increased with increasing loading frequency. Both in the surface-down and surface-up mode, the beams treated with rejuvenator show a higher

bending stiffness. The beams with rejuvenator B show the highest bending stiffness in the SLPA sections. As described before, rejuvenator B is a kind of soft bituminous binder and distributed only in the thin surface layer. That could results in a strong bond between the aggregates at the surface. The bending stiffness in the surface-up mode is relatively higher than surface-down mode. One explanation is that the surface in the rejuvenated area is more rough than the surface in the sawn area.

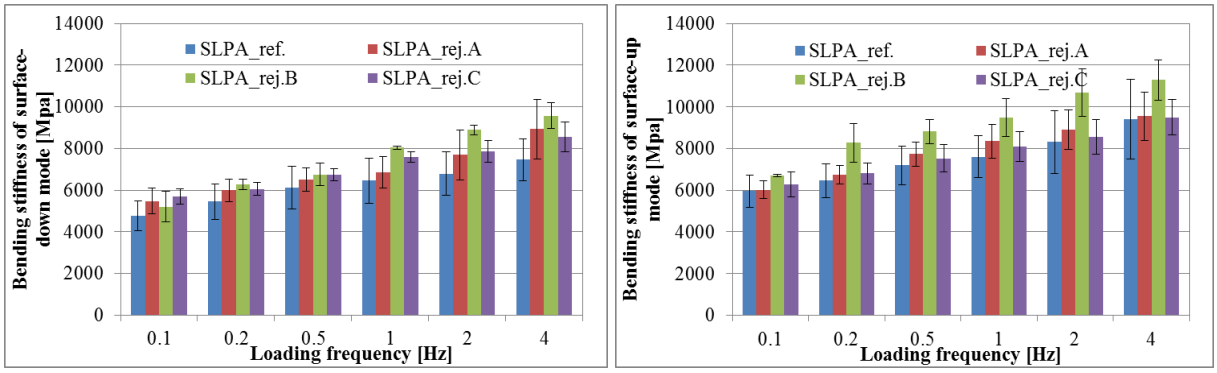

Figure 6: Average of bending stiffness in surface-down and surface-up mode of SLPA beams

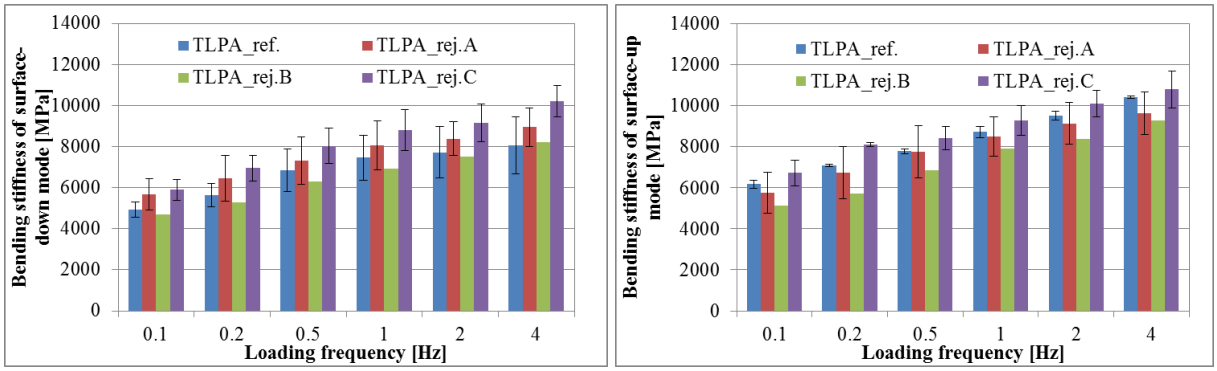

Figure 7: Average of bending stiffness in surface-down and surface-up mode of TLPA beams

Figure 7 show the average values of bending stiffness of TLPA beams. Caution should be given to the results of the beam with rejuvenator B: because only one beam available for testing. For the other sections, the results of two beams were used for calculating the average value. In the surface-down mode of TLPA sections, the reference beams show a lower bending stiffness than treated beams with rejuvenator A and C. Generally the TLPA beams show a higher stiffness than the SLPA beams in this research.

4.3 Beam models

Four cases were modeled for SLPA beam as well as TLPA beam. For case 1, the entire mortar in the beam was assumed to have the same properties (the SBS modified mortar). In case 2, the SBS modified mortar in the top 5 mm was replaced by a soft mortar with a modulus that was 50% of the value of the modulus of the SBS modified mortar. In case 3, no change was made to the mortar, but the voids in the top 5 mm were filled with a soft binder. In case 4, not only the voids in the top 5 mm were filled with a soft binder, but also the SBS modified mortar in the top 5 mm was replaced by a soft mortar as in case 2. Figure 8 shows an example of materials properties of TLPA beam model.

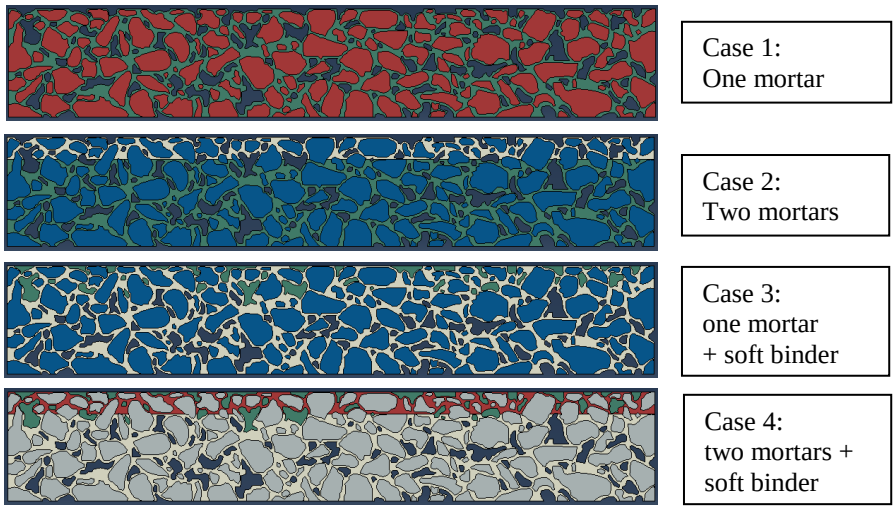

Figure 8: Materials properties of TLPA beam model in different case using segmented color

The maximum deflections of the beams shown in Figure 8 were calculated using ABAQUS. The stiffness of beams was calculated using Equation (1). The results are listed in Table 4. The ratio is the bending stiffness of other cases divided by the bending stiffness of the case 1. The bending stiffness in the surface-down mode is similar to that in the surface-up mode. Two dimensional modeling can't reflect accurately the effects of rejuvenation. However it will give some trends. The results of case 2 indicate that rejuvenation only in top 5 mm of the beam will decrease the bending stiffness of the whole beam. The results of case 3 indicate that applying a binder without assuming rejuvenation will increase the bending stiffness of the whole beam. Case 4 is closest to what happens in practice. On one hand, rejuvenation will soften the mortar resulting in decrease of the bending stiffness. On the other hand, the rejuvenators brings extra binder into the system, this therefore increases the bond between the particles and in consequence increases the bending stiffness.

Table 4: Results of the bending stiffness from the ABAQUS modeling

		SLPA beam model				TLPA beam model			
		Case 1	Case 2	Case 3	Case 4	Case 1	Case 2	Case 3	Case 4
Surface -down	Stiffness [MPa]	26080	23392	29972	27381	24350	20342	31044	26209
	Ratio [%]	--	89.7	114.9	105.0	--	83.5	127.5	107.6
Surface -up	Stiffness [MPa]	26085	23736	29861	27683	24375	20518	30997	26338
	Ratio [%]	--	91.0	114.5	106.1	--	84.2	127.2	108.1

5 CONCLUSIONS

Rejuvenators were sprayed on the porous asphalt pavements in the Netherlands. The influence of the rejuvenators on pavement performance is still being monitored in the LVO project. More results of experimental tests will be reported and published soon. In the research of this paper, it was found that the penetration depth of the rejuvenators varies: rejuvenators applied

as bitumen emulsion and soft binder show a penetration depth of 10 mm and 20 mm in the porous asphalt cores, respectively. The porous asphalt beams from the field show an increased bending stiffness as a result of rejuvenation. The bending stiffness in the surface-up mode is higher than that in the surface-down mode. ABAQUS modeling of beams indicate that rejuvenators not only soften the aged mortar but also give extra binding/bonding to the porous asphalt concrete. The results of ABAQUS modeling prove the increased bending stiffness.

ACKNOWLEDGEMENTS

Some of the research reported in this paper formed part of a research project entitled: 'Lifetime Extension Maintenance of Porous Asphalt (LVO-ZOAB in Dutch)'. The Dutch Ministry of Transport is therefore greatly acknowledge for their permission to use these data.

REFERENCES

Boyer, R.E., 2000. *Asphalt Rejuvenators "Fact, or Fable"*. Prepared for Presentation at the Transportation Systems 2000 (TS2K) Workshop, San Antonio, Texas.

Chiu, C.T. and Lee, M.G., 2006. *Effectiveness of Seal Rejuvenators for Bituminous Pavement Surfaces*. Journal of Testing and Evaluation, 34.

Cooley, L.A., Brumfield, J.W., Mallick, R.B., Mogawer, W.S., Poulikakos, L. and Hicks, G, 2009. *Construction and Maintenance Practices for Permeable Friction Courses*. NCHRP report 640, Transportation Research Board, Washington.

Christensen, D.W. and Anderson, D.A., 1992. *Interpretation of Dynamic Mechanical Test Data for Paving Grade Asphalt Cements.* Journal of the Association of Asphalt Paving Technologists, 61: 67-116.

Estakhri, C.K. and Agarwal, H., 1991. *Effect of Fog seals and Rejuvenators for Bituminous Pavement Surfaces*. Research Report 1156-1F, Texas Department of Transportation, Texas.

Pronk, A.C., 2005. *The Huet-Sayegh Model: A Simples and Excellent Rheological Model for Master Curves of Asphalt Mixes*. Proceedings of the R. Lyttom Symposium on Mechanics of Flexible Pavements, Louisiana, USA.

Qureshi, N.A., Tran, N.H. and Watson, D., 2011. *Effect of Using Fog Seals without Sanding on Surface Friction and Durability of OGFC*. TRB 91st Annual Meeting Compendium of Papers DVD, Transportation Research Board, Washington.

Rogge, D., 2002. *Development of Maintenance Practices for Oregon F-Mix*. FHWA-OR-RD-02-09, Oregon Department of Transportation, Oregon.

Swart, J.H., 1997. *Experience with porous asphalt in the Netherlands*. Proceedings of the European conference on porous asphalt, Madrid, Spain.

Van der Zwan, J.T., Goeman, T., Gruis, H.J.A.J, Swart, J.H. and Oldenburger, R.H., 1990. *Porous Asphalt Wearing Courses in the Netherlands: State of the Art Review*. Transportation Research Record No. 1265, Transportation Research Board, Washington.

Verwaal, W., Zhang, Y. and Chen, F., 2011. *Field trail A50: Year 0 Results of CT Scans*. Report 7-11-185-1, Delft University of Technology, Delft, the Netherlands.

Verwaal, W. and Zhang, Y., 2011. *Field trail A73: Year 0 Results of CT Scans*. Report 7-11-185-7, Delft University of Technology, Delft, the Netherlands.

Woldekidan, M.F., 2012. *Mixture Performance Optimization: Laboratory Investigation and LOT Performance Computations.* Report 7-12-186-2, Delft University of Technology, Delft, the Netherlands.

Woldekidan, M.F., Huurman, M. and Pronk A.C., 2012. *A modified HS model: Numerical applications in modeling the response of bituminous materials*. Finite Elements in Analysis and Design, 53: 37-47.